JCTC Journal of Chemical Theory and Computation

All-Electron Scalar Relativistic Basis Sets for Third-Row Transition Metal Atoms

Dimitrios A. Pantazis,[†] Xian-Yang Chen,[‡] Clark R. Landis,[‡] and Frank Neese*,[†]

Lehrstuhl für Theoretische Chemie, Institut für Physikalische und Theoretische Chemie, Universität Bonn, Wegelerstrasse 12, D-53115 Bonn, Germany, and Department of Chemistry, University of Wisconsin—Madison, 1101 University Avenue, Madison, Wisconsin 53706

Received February 15, 2008

Abstract: A family of segmented all-electron relativistically contracted (SARC) basis sets for the elements Hf−Hg is constructed for use in conjunction with the Douglas−Kroll−Hess (DKH) and zeroth-order regular approximation (ZORA) scalar relativistic Hamiltonians. The SARC basis sets are loosely contracted and thus offer computational advantages compared to generally contracted relativistic basis sets, while their sufficiently small size allows them to be used in place of effective core potentials (ECPs) for routine studies of molecules. Practical assessments of the SARC basis sets in DFT calculations of atomic (ionization energies) as well as molecular properties (geometries and bond dissociation energies for MH_n complexes) confirm that the basis sets yield accurate and reliable results, providing a balanced description of core and valence electron densities. CCSD(T) calculations on a series of gold diatomic compounds also demonstrate the applicability of the basis sets to correlated methods. The SARC basis sets will be of most utility in calculating molecular properties for which the core electrons cannot be neglected, such as studies of electron paramagnetic resonance, Mössbauer and X-ray absorption spectra, and topological analysis of electron densities.

Introduction

Third-row transition metals play important roles in various branches of chemistry. Foremost, they are used in a wide range of catalytic processes including olefin polymerization and numerous forms of hydrocarbon functionalization. In a biological context, tungsten is the only naturally occurring third-row transition element. It is found in a number of enzyme active sites, where it usually catalyzes redox reactions similar to those performed by the analogous molybdenum enzymes.[1,2] The biologically relevant redox states are W(IV), W(V), and W(VI) where only W(V) is amenable to electron paramagnetic resonance (EPR) studies owing to the $5d^1$ electron configuration. However, other third-row transition metals like osmium, gold, platinum, and rhenium are sometimes also used in a biological context, the long-established medicinal applications of platinum and gold compounds being prominent examples.[3]

In recent years, it has become commonplace to supplement experimental studies by quantum chemical calculations that are designed to assist in the interpretation of experimental data or to provide information where experiments cannot be performed with realistic effort. The emphasis of most calculations, commonly performed at some level of density functional theory (DFT),[4,5] is on the relative energies of reactants, products, transition states, isomers, or conformers. A potential problem in calculations on third-row transition elements is the relatively high computational effort required to treat all the inner shell electrons (1s−4f) together with the importance of relativistic effects that are certainly not negligible in the third transition row.[6] As long as only energetics is concerned it has therefore been found to be convenient to employ effective core potentials (ECPs).[7–17] Properly designed ECPs together with suitable valence basis sets fulfill the double purpose of decreasing the computational

* Corresponding author. E-mail: neese@thch.uni-bonn.de.
[†] Universität Bonn.
[‡] University of Wisconsin—Madison.

10.1021/ct800047t CCC: $40.75
Published on Web 05/08/2008

effort—since only valence electrons are explicitly considered—as well as incorporating scalar relativistic effects. The calculations then proceed as in the nonrelativistic case.[18]

In various assessments and practical applications, it has been established that ECPs provide reliable approximations to all-electron scalar relativistic calculations as far as geometries and relative energies are concerned.[19] By contrast, obvious limitations arise when properties of the inner shells are being probed, as is the case in EPR or X-ray absorption experiments. At the very least for such cases, there should be basis sets available that allow scalar relativistic calculations with realistic effort, being adapted to the popular formulations of scalar relativistic Hamiltonian operators, such as the zeroth-order regular approximation[20–23] (ZORA), the infinite-order regular approximation[24] (IORA), and the Douglas−Kroll−Hess[25–29] (DKH) approach. It is common practice in basis set design to use a single contracted basis function for each core orbital since these orbitals undergo very limited changes upon bond formation. Unfortunately, different scalar relativistic approximations lead to very different shapes of the core orbitals and hence require contractions that are quite different from each other and from the nonrelativistic case. Therefore, standard contracted basis sets generally lack the flexibility in the core region for scalar relativistic methods and although uncontracted basis sets provide greater flexibility, their large size makes routine molecular calculations too slow to be practical.

Scalar relativistic basis sets for the ZORA approximation have been developed by the Amsterdam group for Slater functions and are available in the Amsterdam Density Functional code.[30,31] Van Wüllen has performed scalar relativistic contractions for the ZORA approximation, but to the best of our knowledge, his basis sets are not publicly available.[32] Various workers have recently reported basis sets for transition metal atoms that are contracted to be consistent with the second- or third-order DKH (DKH2, DKH3) procedures.[33–40] Representative examples are the atomic natural orbital (ANO) basis sets by the Lund group,[33] the correlation consistent basis sets for the first transition row developed by Peterson and co-workers[34] and the comprehensive basis sets proposed by Nakajima and Hirao[35] and by Koga and co-workers.[36–38] These basis sets are generally contracted and hence, as long as the integral generator of a given quantum chemical program does not take advantage of the general contraction, lead to fairly expensive calculations. This is not so much an issue in correlated ab initio calculations for which these basis sets were designed. It nevertheless becomes a serious efficiency issue for DFT calculations where the generation of two-electron integrals over basis functions dominates the computational effort.

Hence, we feel that it is important to have basis sets available that are not generally contracted but that can be used in scalar relativistic calculations. In this paper we propose such segmented all-electron relativistically contracted (SARC) basis sets, which are constructed for treatments of third-row transition metal systems in conjunction with scalar relativistic Hamiltonians (DKH or ZORA), yet are sufficiently small to be used in place of effective core potentials (ECPs) for routine studies of molecules. Exponents of the Gaussian primitives are derived from relatively simple empirical rules and contraction coefficients were determined in atomic complete active space self-consistent field (CASSCF) calculations in both the ZORA and second-order DKH (DKH2) schemes. In order to arrive at consistent sets of all-electron scalar relativistic basis sets covering most of the periodic table, we have furthermore recontracted the basis sets developed by the Karlsruhe group[41–43] along the same lines. Thus, basis sets of split-valence (SV), triple-ζ-valence (TZV), and quadruple-ζ-valence (QZV) quality are available in ZORA and DKH recontractions and can be combined with the SARC basis sets for third-row transition metals. All the above basis sets are now part of the freely available ORCA program package.[44] Scalar relativistic ZORA and DKH2 calculations based on the SARC basis sets are only slightly more expensive than standard nonrelativistic calculations and are not grossly less efficient than calculations that employ ECPs as long as the number of heavy atoms in the system is not too large. The performance of the SARC basis sets is assessed for both atomic properties (ionization energies) and molecular properties (structures and bond dissociation energies for MH_n complexes with less than 12 valence electrons).

Relativistic Hamiltonians

In this section, the well-known[45,46] underlying relativistic formalisms are briefly described. The reasoning starts with the four-component Dirac−Coulomb many electron Hamiltonian that consists of the one-electron Dirac Hamiltonian supplemented by the standard nonrelativistic electron−electron interaction terms. Calculations that are directly based on this Hamiltonian are feasible—as implemented in the Dirac code[47]—but are still computationally expensive. Much effort has been devoted to develop theories that decouple the large and small components of the four-component Dirac spinors. The earliest of these, the Breit−Pauli expansion, is known to face the variational collapse problem[45,46] and has therefore fallen into disuse in the framework of variational calculations.

The zeroth-order regular approximation (ZORA) is an effective Hamiltonian approach that was first discussed by Heully and co-workers[48,49] and later elaborated by van Lenthe et al.[20–22] Various modifications have been discussed by van Wüllen[23] and Filatov.[50–54] The ZORA method amounts to an expansion of the Dirac equation in powers of $E/(2c^2 - V)$ where V is the "molecular potential" and E is the Dirac energy. To leading order, the energy dependence does not appear. In a Kohn−Sham framework, the ZORA Hamiltonian is of the form $\{(c\boldsymbol{\sigma}\mathbf{p})[1/(2c^2 - V)](c\boldsymbol{\sigma}\mathbf{p}) + V\}\psi_i = \varepsilon_i\psi_i$, with $\boldsymbol{\sigma}$ representing the vector of Pauli spin-matrices[45] and $\mathbf{p}$ being the momentum operator.

The Douglas−Kroll−Hess (DKH) method represents an alternative way for decoupling the Dirac Hamiltonian. It is based on a series of unitary transformations, the first of which is the free particle Fouldy−Wouthuysen transformation.[55] The series apparently converges very fast and is usually truncated at second-order, which yields good results. Reiher and Wolf[55–61] have extensively developed and discussed higher-order terms in the DKH series. Other discussions of third-[62] and sixth-order[63] terms have also appeared in the literature. The equations are fairly complex and will not be

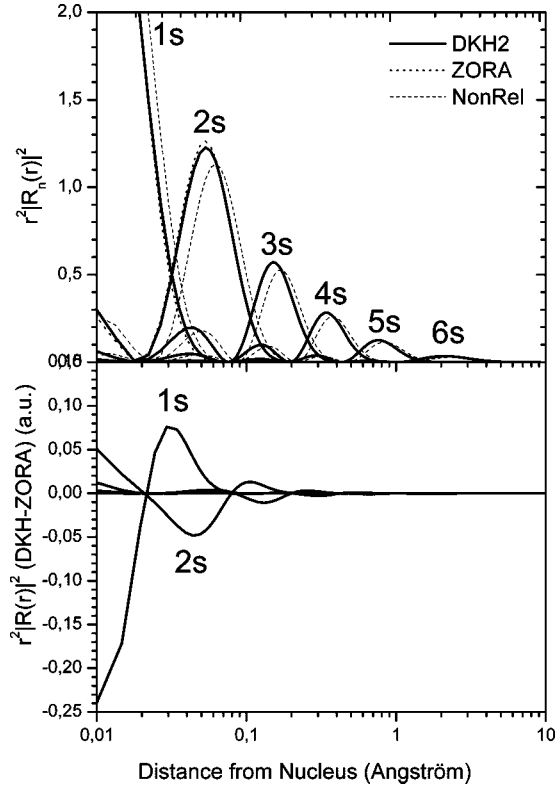

Figure 1. (top) Radial distribution functions of the neutral Hg atom (^{1}S) in the DKH2 (full line), ZORA (dotted line), and nonrelativistic (dashed line) approximations. (bottom) Difference between the DKH and ZORA radial distribution functions. All calculations were done at the RHF level with the decontracted WTBS basis set.

provided here. In programmable form, they have as examples been given in refs 56 and 59. More recently, high-order and even exact decoupling procedures have been discussed by various authors[57,60,64–68] and will likely find their way into major quantum chemistry codes in the future.

Once the reduction of the Dirac equation to two components has been achieved, it can be conveniently (but not uniquely)[69] divided into a spin-dependent and a spin-independent part using the well-known Dirac relation $(\boldsymbol{\sigma}\mathbf{u})(\boldsymbol{\sigma}\mathbf{v}) = \mathbf{uv} + i\boldsymbol{\sigma}(\mathbf{u} \times \mathbf{v})$ that holds for any two vectors $\mathbf{u}$, $\mathbf{v}$ that are independent of $\boldsymbol{\sigma}$. If the spin-dependent part (the spin−orbit coupling) is dropped, or taken into account perturbationally at a later stage, one arrives at a spin-free effective one-component method that typically only features a modified one-electron part of the Hamiltonian. This is the approach taken in this work. However, the effective one-electron Hamiltonians differ according to the chosen method of decoupling. Since the effective potentials provided by different decoupling procedures are quite different, it is necessary to use different contraction schemes for different methods. Hence, it is necessary to determine the all-electron contractions for each scalar-relativistic Hamiltonian separately.

The difference in radial functions is illustrated in Figure 1, where the radial functions of the s orbitals of the neutral Hg atom (^{1}S) are displayed. As is well-known, the relativistic and nonrelativistic orbitals are significantly different and all radial maxima of the nonrelativistic calculation appear at considerably too long distances. Compared to this major difference, the ZORA and DKH2 orbitals are relatively similar. The difference plot reveals that the only significant differences occur in the 1s and 2s orbitals. The ZORA 1s orbital is more compact than the DKH2 orbital and consequently shifted inward. The same effect is observed for the 2s orbital where the dominant radial maximum occurs at slightly shorter distances in the ZORA calculation, but in the region close to the nucleus, the DKH 2s orbital is larger. This is related to the orthogonality constraint of the 2s and 1s orbitals. The behavior of the DKH2 and ZORA orbitals is understood from the well-known fact that the deep core-orbital energies are much too low in the ZORA method.[20] Thus, the ZORA potential is too attractive close to the nucleus. This will ultimately have influence on deep core properties, but the valence region is described very similarly by both relativistic methods.

Table 1. Radial Expectation Values (in Bohr) Determined from CASSCF Calculations

	$\langle r_s \rangle$	$\langle r_p \rangle$	$\langle r_d \rangle$	$\langle r_f \rangle$
Hf	0.021044	0.075387	0.190489	0.638176
Ta	0.020753	0.074278	0.187201	0.607539
W	0.020470	0.073201	0.184024	0.580906
Re	0.020195	0.072155	0.180953	0.557585
Os	0.019927	0.071138	0.177983	0.536501
Ir	0.019666	0.070149	0.175109	0.517408
Pt	0.019411	0.069188	0.172325	0.500012
Au	0.019164	0.068253	0.169628	0.484067
Hg	0.018922	0.067342	0.167014	0.469201

Construction of Basis Sets

CASSCF calculations (or restricted Hartree−Fock (RHF) for d^{10} ^{1}S states) were first carried out for each atom in order to obtain the innermost radial expectation values to be used in the generation of the new primitives. These calculations employed Huzinaga's well-tempered basis sets (WTBS)[70,71] in completely uncontracted form (28s21p18d12f), resulting in a total of 265 basis functions per atom except for Hg, for which the basis set is (29s21p19d13f) with a total of 278 basis functions. Each atom was considered in its ground state, with the exceptions of rhenium, for which we averaged with equal weights the lowest sextet state arising from each of $5d^56s^2$ and $5d^66s^1$ configurations, and osmium, for which we used the lowest state of the $5d^76s^1$ configuration. Specifically, the states of the atoms were: Hf (^{3}F), Ta (^{4}F), W (^{5}D), Re (^{6}S, ^{6}D), Os (^{5}F), Ir (^{4}F), Pt (^{3}D), Au (^{2}S), and Hg (^{1}S).

On the basis of the innermost radial expectation values $\langle r_l \rangle$ determined from the above calculations (Table 1), the maximal exponents per angular momentum α_l (l = s, p, d, f), i.e. the exponents of the tightest functions were then determined according to the formula:

$$\alpha_l = k_l \frac{2f_l^2}{\pi \langle r_l \rangle^2} \tag{1}$$

where f_l assumes the values of 1, 4/3, 8/5, and 64/35, and κ_l is a scaling factor, whose optimal values were determined to be 1000, 100, 33, and 10 for s, p, d, and f functions, respectively. The results are summarized in Table 2. Having

Table 2. Maximum Exponents Per Angular Momentum (in Bohr^{-2}) Used in the SARC Basis Sets

	α_s	α_p	α_d	α_f
Hf	1437551.912320	19914.282978	1482.157051	52.266455
Ta	1478149.466003	20513.378492	1534.679527	57.670758
W	1519303.147809	21121.442157	1588.126510	63.080083
Re	1560962.277531	21738.257763	1642.488936	68.467082
Os	1603231.663005	22364.247712	1697.762680	73.954211
Ir	1646069.065505	22999.300491	1753.949530	79.512920
Pt	1689601.567586	23642.643991	1811.079246	85.141859
Au	1733435.947505	24294.843503	1869.127577	90.843326
Hg	1778058.504339	24956.609026	1928.094310	96.691016

determined the maximum exponents, series of descending primitives were then generated as $\alpha_i\chi^{-i}$ (i is a positive integer), χ being 2.25, 2.50, 2.75, and 3.00, for s, p, d, and f. Extrapolation factors were chosen empirically in an attempt to produce the smallest possible set of primitives that does not compromise appreciably the accuracy in the valence region. Each series was terminated when the exponent became smaller than 0.05 for s, p, and d functions or 0.5 for f functions; this procedure yielded (22s15p11d6f) sets with a total of 164 primitives. From these, the innermost 6s, 5p, 4d, and 5 or 4f primitives were contracted in the final basis sets, leaving the remaining primitives uncontracted. Contraction coefficients were obtained through scalar relativistic CASSCF calculations using the same states for each atom as described above, except for Re and Os that were now also considered in their respective ground states, ^{6}S and ^{5}D. Distinct sets of contraction coefficients were determined depending on the treatment of scalar relativistic effects: the basis sets therefore exist in two forms, one optimized for the DKH2 Hamiltonian and one optimized for the ZORA approximation.

When the SARC basis sets are used in conjunction with SV basis sets, the f primitives are contracted in a [51] pattern, whereas a [411] pattern is used when combined with TZV basis sets. Finally, for use with more extensively polarized TZVPP basis sets or for correlated methods, the SARC basis sets are supplemented with an additional single g function taken from a def2-TZVPP basis.[42] Thus, the final contraction patterns and total basis functions for the SARC basis sets in the SV/SVP, TZV/TZVP, and TZVPP forms are [17s11p8d2f] (104 functions), [17s11p8d3f] (111 functions), and [17s11p8d3f1g] (120 functions), respectively. Complete listings of the basis sets are included in the Supporting Information.

As mentioned in the Introduction, we also produced DKH and ZORA relativistically contracted variants of the Karlsruhe SV, TZV (H−Xe), and QZV (H−Kr) basis sets,[41–43] in order to ensure consistency when these are combined with the SARC basis sets for third-row transition metals. A much simpler procedure was followed in this case as the original exponents were not altered. However, new contraction coefficients were determined following CASSCF calculations with completely uncontracted basis sets. It is emphasized that only the innermost primitives per angular momentum were recontracted, hence the relativistic SV, TZV, and QZV variants are slightly larger than the original nonrelativistic basis sets. These basis sets are automatically loaded in place of the SV, TZV, or QZV basis sets when the use of a scalar relativistic Hamiltonian is detected.

Table 3. Estimated Incompleteness Errors (E_h) from Comparison of the SARC and Uncontracted WTBS Basis Sets[a]

	unc WTBS	SARC	ΔE
Hf	−15064.0138878	−15059.7917292	4.2221586
Ta	−15589.9018509	−15585.3767151	4.5251358
W	−16127.3776871	−16122.5137047	4.8639824
Re	−16676.6130872	−16671.3706773	5.2424099
Os	−17237.6115677	−17231.9529489	5.6586188
Ir	−17810.6802821	−17804.5642806	6.1160015
Pt	−18395.9799302	−18389.3624406	6.6174896
Au	−18993.6960534	−18986.5266065	7.1694469
Hg	−19603.8631097	−19596.1093860	7.7537237

[a] Calculations were done at the CASSCF level of theory with the DKH2 Hamiltonian.

Preliminary Considerations

The particular choice of the contraction pattern in the SARC basis sets was guided by the need to strike a balance between reduced basis set size and reliable results. An estimation of the contraction error is therefore necessary in order to establish whether the contraction pattern is uniformly good or leads to specific failures. The contraction error is obtained as the difference between total CASSCF energies for the same atomic states calculated with the contracted and fully uncontracted versions of the basis sets. Specifically, DKH2 calculations with the SARC [17s11p8d3f] basis sets indicate that the contraction error is of the order of 0.1 E_h and shows no irregular deviations: it increases monotonically from a minimum of 79 mE_h for hafnium to a maximum of 121 mE_h for mercury, while 70−80% of the energy difference between the contracted and uncontracted basis sets was found to originate in the p contraction. Essentially, identical trends and numerical values are obtained from the corresponding ZORA energies. These results confirm the uniform validity of the chosen contraction pattern across the third transition metal row.

To put the numbers mentioned above into perspective, we note that the contraction error is insignificant compared to the inherent incompleteness error relative to the basis set limit. This is shown clearly in Table 3, where total electronic energies obtained with SARC are compared to those obtained with the fully uncontracted WTBS, the latter being a good approximation to an essentially complete basis set. A rising trend in deviations is observed again as we move from the lighter to the heavier atoms, the incompleteness error ranging from a little over 4 E_h for hafnium to 7.75 E_h for mercury. Crucially, however, these relatively large absolute differences are not expected to have any adverse effects on the prediction of molecular properties other than total energies. This point is more meaningfully demonstrated by comparison of the valence shell orbital energies obtained with the two basis sets: regardless of the incompleteness error, the energies of the 5d and 6s orbitals are shifted by only a few hundredths of an electronvolt relative to the uncontracted WTBS energies (average 0.066 eV) and they never exceed 0.1 eV for any metal. Moreover, the lack of periodic trends in this case

Table 4. Ionization Energies (eV) Computed with the B3LYP Functional and the Fully Uncontracted WTBS Basis Set, with and without Relativistic Corrections, Compared to Experimental Values

		nonrelativistic		DKH2		ZORA	
	exp[a]	IE	ΔE	IE	ΔE	IE	ΔE
Hf	6.825	6.714	−0.111	6.721	−0.104	6.726	−0.099
Ta	7.550	6.633	−0.916	7.472	−0.077	7.489	−0.061
W	7.864	5.977	−1.887	7.791	−0.073	7.808	−0.056
Re	7.834	6.925	−0.909	7.916	0.083	7.936	0.102
Os	8.438	8.998	0.560	8.476	0.038	8.490	0.052
Ir	8.967	10.101	1.134	8.895	−0.072	8.901	−0.066
Pt	8.959	7.290	−1.669	9.163	0.204	9.193	0.234
Au	9.226	7.321	−1.904	9.347	0.121	9.380	0.155
Hg	10.438	8.419	−2.019	10.319	−0.118	10.354	−0.083
MUE			1.234		0.099		0.101
rms			1.387		0.109		0.115

[a] Reference 72.

confirms that the basis sets yield a valence description of consistent quality across the transition row. For the chemically less important 4f and 5s orbitals, the energy differences are slightly more pronounced, but still they only exceed 0.2 eV for the three heaviest elements. Overall, the mean absolute deviation for the 4f−6s orbital energies averaged over all metals amounts to 0.106 eV. Thus, despite the considerable size reduction in the SARC basis sets (111 instead of 265 functions), the description of the valence region in orbital energetic terms is essentially unaltered; the importance of this will be demonstrated in the following sections detailing practical assessments for both atomic and molecular systems.

Ionization Energies. Reliable prediction of atomic ionization energies is a typical requirement for computational methods both because it is an obvious measure of the balanced treatment of different electronic configurations and because it often reflects on the performance of the method for molecular environments. With the exception of hafnium, the first ionization energy originates in the removal of an electron from the 6s orbital of the neutral atom, as might be anticipated. The resulting electronic configurations and ground states of the cations are then as follows: Hf^+ (d^1s^2, ^2D), Ta^+ (d^3s^1, ^5F), W^+ (d^4s^1, ^6D), Re^+ (d^5s^1, ^7S), Os^+ (d^6s^1, ^6D), Ir^+ (d^7s^1, ^5F), Pt^+ (d^9s^0, ^2D), Au^+ ($d^{10}s^0$, ^1S), and Hg^+ ($d^{10}s^1$, ^2S). Since the SARC basis sets were developed with the intention to be used in routine molecular studies where DFT currently dominates or is the only cost-effective option, we chose to carry out the present assessment using the popular B3LYP functional.

Complete neglect of relativity leads in general to severe underestimation of ionization energies, with a root-mean-squared (rms) error of 1.4 eV and nonsystematic individual errors that can reach 2 eV (Table 4). Inclusion of scalar relativistic effects reduces these deviations dramatically, bringing the rms error down to 0.11 eV. Pt presents the greatest error, its ionization energy being overestimated by more than 0.2 eV. The ZORA and DKH results are essentially of the same quality. Most importantly, the transition from the uncontracted WTBS to the much more compact SARC (Table 5) has minimal impact on the accuracy of the computed values, the rms error increasing by a mere 0.01 eV. The graphical comparison of experimental and calculated ionization energies in Figure 2 shows vividly how closely the predicted values follow experiment, with Pt producing again the only significant deviation. This outcome demonstrates not only the quality of the SARC basis sets, but also the excellent performance of the B3LYP functional: the rms error of 0.12 eV for the third transition metal series matches that reported by Roos et al. for CASPT2 with a much more extended relativistic ANO basis set.[33]

Table 5. Ionization Energies (eV) Computed with the B3LYP Functional and the SARC Basis Sets, Compared to Experimental Values

		DKH2		ZORA	
	exp	IE	ΔE	IE	ΔE
Hf	6.825	6.711	−0.115	6.716	−0.109
Ta	7.550	7.466	−0.084	7.481	−0.069
W	7.864	7.791	−0.073	7.807	−0.057
Re	7.834	7.915	0.081	7.933	0.099
Os	8.438	8.483	0.045	8.503	0.065
Ir	8.967	8.896	−0.071	8.904	−0.063
Pt	8.959	9.197	0.238	9.223	0.264
Au	9.226	9.382	0.157	9.412	0.186
Hg	10.438	10.342	−0.096	10.373	−0.065
MUE			0.107		0.108
rms			0.120		0.128

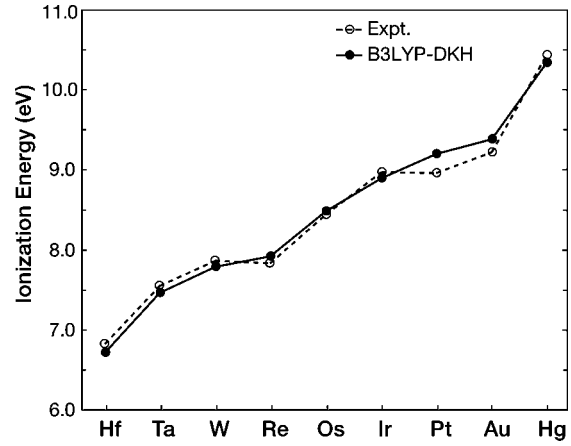

Figure 2. Comparison between experimental and computed (B3LYP-DKH2) first ionization energies.

Molecular Tests

The calculation of molecular properties such as geometries and bond dissociation enthalpies is an essential application of modern electronic structure theory. Third-row transition metal hydrides having the formula MH_n, for which the total valence electron count does not exceed 12,[73–76] constitute a computationally accessible set for testing the influence of relativistic effects on molecular properties. Such complexes have been examined recently by Landis and co-workers[77] using effective core potentials and their associated contracted valence basis sets, providing a useful comparison set for the basis sets described herein. These metal hydride complexes have electronic structures that are compatible with simple Lewis-like formulations,[73] and natural bond orbital (NBO) analysis[73,78–84] of their electronic structures using both SARC and uncontracted basis sets with different scalar relativistic treatments probes the robustness of simple Lewis-like

Table 6. Geometric Data and Total Energies of MH_n and MH_{n-1} Compounds at the B3LYP Level with Uncontracted (UC) and Contracted (C) SARC Basis Sets, Using the DKH and ZORA Hamiltonians

MH_n	point group	basis set	M−H bond (Å)	H−M−H angle (deg)	total energies (E_h)
HfH_4	T_d	UC-SARC-DKH	1.835	109.56	−15067.61713715
		C-SARC-DKH	1.841	109.56	−15067.52054279
		UC-SARC-ZORA	1.832	109.47	−15650.32180781
		C-SARC-ZORA	1.837	109.47	−15650.20652157
	C_{4v}	UC-SARC-DKH	1.814	78.42	−15067.55910933
		C-SARC-DKH	1.820	78.29	−15067.46219894
		UC-SARC-ZORA	1.813	78.58	−15650.26167290
		C-SARC-ZORA	1.819	78.42	−15650.14619041
HfH_3	C_{3v}	UC-SARC-DKH	1.848	119.13	−15066.98814663
		C-SARC-DKH	1.853	119.11	−15066.89160658
		UC-SARC-ZORA	1.845	119.15	−15649.69245223
		C-SARC-ZORA	1.850	119.13	−15649.57717761
TaH_5	C_{4v}	UC-SARC-DKH	1.744, 1.792	77.64/117.55	−15593.84558554
		C-SARC-DKH	1.751, 1.797	77.66/117.53	−15593.74525223
		UC-SARC-ZORA	1.746, 1.781	77.79/117.38	−16213.94501662
		C-SARC-ZORA	1.752, 1.788	77.69/117.50	−16213.82508781
	C_{2v}	UC-SARC-DKH	1.712, 1.746,1.782	63.82, 117.90	−15593.84302285
		C-SARC-DKH	1.718, 1.752, 1.787	63.75, 117.93	−15593.74260863
		UC-SARC-ZORA	1.716, 1.747,1.773	63.7, 117.61	−16213.94250329
		C-SARC-ZORA	1.722, 1.753,1.779	63.71, 117.70	−16213.82243700
TaH_4	T_d	UC-SARC-DKH	1.766	109.54	−15593.23874364
		C-SARC-DKH	1.772	109.54	−15593.13848434
		UC-SARC-ZORA	1.762	109.50	−16213.33985941
		C-SARC-ZORA	1.768	109.50	−16213.21979555
	C_{4v}	UC-SARC-DKH	1.748	78.13	−15593.21134922
		C-SARC-DKH	1.755	78.12	−15593.11108567
		UC-SARC-ZORA	1.750	78.33	−16213.31044183
		C-SARC-ZORA	1.756	78.31	−16213.19054552
WH_6	C_{3v}	UC-SARC-DKH	1.652, 1.708	63.24, 113.5	−16131.64727768
		C-SARC-DKH	1.657, 1.713	63.16, 113.6	−16131.54346908
		UC-SARC-ZORA	1.658, 1.705	63.38, 113.3	−16791.11504169
		C-SARC-ZORA	1.663, 1.709	63.34, 113.3	−16790.99057155
WH_5	C_{2v}	UC-SARC-DKH	1.665, 1.681,1.720	62.36, 116.44	−16131.03550734
		C-SARC-DKH	1.671, 1.687,1.724	62.31, 116.40	−16130.93176895
		UC-SARC-ZORA	1.670, 1.684,1.712	62.26, 116.29	−16790.50733939
		C-SARC-ZORA	1.676, 1.689,1.717	62.24, 116.28	−16790.38274965
	C_{4v}	UC-SARC-DKH	1.744, 1.677	76.54/118.91	−16131.03530403
		C-SARC-DKH	1.748, 1.683	76.50/118.95	−16130.93144660
		UC-SARC-ZORA	1.732, 1.681	76.61/118.72	−16790.50659133
		C-SARC-ZORA	1.736, 1.686	76.60/118.75	−16790.38195088
	C_{5v}	UC-SARC-DKH	1.672	64.86	−16131.01858750
		C-SARC-DKH	1.677	64.77	−16130.91477084
		UC-SARC-ZORA	1.673	64.82	−16790.48867413
		C-SARC-ZORA	1.678	64.81	−16790.36407530
ReH_5	C_{5v}	UC-SARC-DKH	1.620	62.99	−16679.90974069
		C-SARC-DKH	1.625	62.97	−16679.80333331
		UC-SARC-ZORA	1.623	63.17	−17380.81762186
		C-SARC-ZORA	1.627	63.19	−17380.68863645
	C_{4v}	UC-SARC-DKH	1.695, 1.616	76.12/119.33	−16679.90681889
		C-SARC-DKH	1.699, 1.621	76.09/119.43	−16679.79954812
		UC-SARC-ZORA	1.682, 1.621	76.23/119.21	−17380.81524275
		C-SARC-ZORA	1.686, 1.626	76.20/119.23	−17380.68542780
	C_{2v}	UC-SARC-DKH	1.640, 1.612,1.654	116.99, 56.95, 65.81	−16679.90890282
		>C-SARC-DKH	1.647, 1.616,1.658	116.53, 56.55, 65.93	−16679.80201210
		UC-SARC-ZORA	1.643, 1.617,1.650	116.47, 56.14, 66.32	−17380.81861597
		C-SARC-ZORA	1.648, 1.621,1.655	116.28, 55.72, 66.50	−17380.68910645
ReH_4	T_d	UC-SARC-DKH	1.644	109.13	−16679.30977871
		C-SARC-DKH	1.648	109.70	−16679.20326767
		UC-SARC-ZORA	1.642	109.47	−17380.22240021
		C-SARC-ZORA	1.647	109.47	−17380.09310021
	C_{4v}	UC-SARC-DKH	1.617	68.49/76.73	−16679.29524772
		C-SARC-DKH	1.622	68.38/76.94	−16679.18850066
		UC-SARC-ZORA	1.622	68.40/79.13	−17380.20339418
		C-SARC-ZORA	1.627	68.43/79.17	−17380.07408378
OsH_4	T_d	UC-SARC-DKH	1.592	109.47	−17240.05827094
		C-SARC-DKH	1.597	109.47	−17239.94858367
		UC-SARC-ZORA	1.591	109.47	−17984.56862903
		C-SARC-ZORA	1.595	109.47	−17984.43496057

Table 6. Continued

MH_n	point group	basis set	M−H bond (Å)	H−M−H angle (deg)	total energies (E_h)
	C_{4v}	UC-SARC-DKH	1.562	71.04	−17240.05287730
		C-SARC-DKH	1.567	71.09	−17239.94267012
		UC-SARC-ZORA	1.569	72.25	−17984.55665962
		C-SARC-ZORA	1.573	72.23	−17984.42277243
OsH_3	C_{3v}	UC-SARC-DKH	1.588	104.98	−17239.43763702
		C-SARC-DKH	1.593	105.15	−17239.32799126
		UC-SARC-ZORA	1.589	105.24	−17983.94753645
		C-SARC-ZORA	1.593	105.37	−17983.81389535
IrH_3	C_{3v}	UC-SARC-DKH	1.534	87.67	−17812.20363055
		C-SARC-DKH	1.538	88.04	−17812.09019536
		UC-SARC-ZORA	1.539	91.47	−18602.56588914
		C-SARC-ZORA	1.543	91.49	−18602.42677137
IrH_2		UC-SARC-DKH	1.542	88.11	−17811.57595938
		C-SARC-DKH	1.546	88.51	−17811.46295422
		UC-SARC-ZORA	1.547	92.81	−18601.93950386
		C-SARC-ZORA	1.550	92.92	−18601.80067284
PtH_2		UC-SARC-DKH	1.510	82.56	−18396.49795977
		C-SARC-DKH	1.514	82.75	−18396.38120805
		UC-SARC-ZORA	1.515	86.80	−19235.07546132
		C-SARC-ZORA	1.518	86.77	−19234.93083937
PtH		UC-SARC-DKH	1.527		−18395.86957063
		C-SARC-DKH	1.530		−18395.75344984
		UC-SARC-ZORA	1.530		−19234.44728022
		C-SARC-ZORA	1.533		−19234.30312472
AuH		UC-SARC-DKH	1.537		−18993.10537990
		C-SARC-DKH	1.541		−18992.98480346
		UC-SARC-ZORA	1.538		−19882.38086053
		C-SARC-ZORA	1.539		19882.23043055
Au		UC-SARC-DKH			−18992.49444792
		C-SARC-DKH			−18992.37453488
		UC-SARC-ZORA			−19881.76785321
		C-SARC-ZORA			−19881.61798680
H		UC-SARC-DKH			−0.49876441
		C-SARC-DKH			−0.49875809
		UC-SARC-ZORA			−0.49877893
		C-SARC-ZORA			−0.49877160

structures to more complete descriptions of the electron density distributions. The comprehensive comparison of the computed X−MH_n bond dissociation energies that was performed using B3LYP and CCSD(T) methods with relativistic effective core potentials[77] is also of great relevance for our present assessment. In the following, we assess the performance of the all-electron SARC basis sets in both DKH and ZORA scalar relativistic approaches comparing the results with this wide array of important molecular properties such as structure and bond dissociation enthalpies along with chemically meaningful interpretations such as charge distributions and orbital hybridizations.

MH_n Computational Details. All calculations were performed using either ORCA[44] or ADF 2005.[31,85–88] In ORCA calculations, a full geometry optimization for each structure was performed using the hybrid density functional B3LYP method.[89,90] Scalar relativistic corrections were included using the Douglas−Kroll−Hess (DKH2) and zeroth-order regular approximation (ZORA) methods with the option "onecenter true" enabled. The all-electron SARC basis sets were used in both contracted (17s11p8d2f) and uncontracted (22s15p11d6f) form for all transition metal elements. The SCF convergence threshold was set to VeryTight and the natural population anaysis (NPA)[80,81,83] was performed using the interface of ORCA to the GenNBO program version 5.0 on the geometries optimized at the B3LYP/uncontracted-SARC level. For ADF 2005 calculations, the density functional used was based on Vosko−Wilk−Nusair (VWN)[91] local-spin-density correlated potential with gradient corrections of the exchange correlation due to Perdew and Wang (PW91).[92] The frozen-core approximation was adopted for M shells ($1s^2 \rightarrow 4d^{10}$). The core electrons were calculated by the accurate relativistic Dirac−Slater method[93] and then transferred unchanged into the molecules. The valence orbitals of H and transition metal

Table 7. Natural Population Analysis (NPA) Charges on M (Q_M) and H (Q_H) Computed for the Most Stable MH_n and MH_{n-1} Species at the B3LYP Level with the SARC Basis Sets and the DKH2 Hamiltonian

compounds	point group	Q_M	Q_H
HfH_4	T_d	1.774	−0.444
HfH_3	C_{3v}	1.453	−0.484
TaH_5	C_{4v}	1.357	−0.348, −0.254
TaH_4	T_d	1.317	−0.329
WH_6	C_{3v}	0.481	−0.002, −0.158
WH_5	C_{2v}	0.748	−0.056, −0.214, −0.133
ReH_5	C_{5v}	−0.069	0.014
ReH_4	T_d	0.460	−0.115
OsH_4	T_d	0.088	−0.022
OsH_3	C_{3v}	0.125	−0.042
IrH_3	C_{3v}	−0.176	0.058
IrH_2	C_{2v}	−0.007	0.004
PtH_2	C_{2v}	−0.152	0.076
PtH		0.024	−0.024
AuH		0.047	−0.047

Table 8. Computed Bond Dissociation Energies (kcal/mol) at Various Levels of Theory for the Most Stable Neutral, Valence-Saturated MH_n Compounds at Geometries Optimized for Each Method

	B3LYP					CCSD(T)	PW91
	UC-SARC DKH	C-SARC DKH	UC-SARC ZORA	C-SARC ZORA	lacv3p++** [a]	lacv3p++** [a]	TZ2P-ZORA
HfH_4	81.72	81.69	81.94	81.93	81.59	73.90	79.11
TaH_5	67.82	67.78	66.75	66.84	70.06	66.6	66.6
WH_6	70.91	70.87	68.35	68.43	67.78	66.15	72.01
ReH_5	63.50	63.57	60.52	60.72	62.22	62.22	67.67
OsH_4	76.47	76.45	76.75	76.74	77.9	78.67	77.22
IrH_3	80.89	80.62	80.07	80.08	80.29	80.29	84.45
PtH_2	81.34	80.95	81.20	80.91	80.92	83.81	85.12
AuH	70.38	69.97	71.68	71.33	71.00	–	77.82

[a] Previously reported.[77]

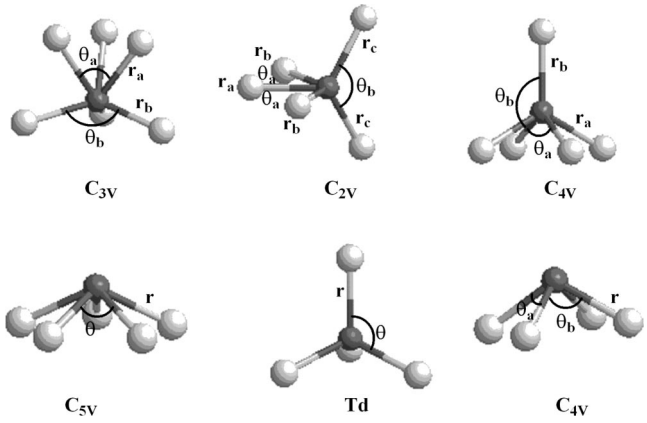

Figure 3. Illustrations of some energy minimized structures for MH_n complexes ($n = 4, 5, 6$).

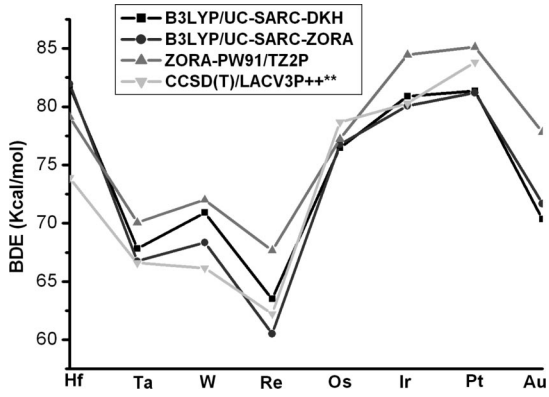

Figure 4. Single bond dissociation energies (BDE, kcal/mol) of $H-MH_{n-1}$ complexes along the third-row transitional metal at the B3LYP level with SARC-DKH and SARC-ZORA basis sets and ZORA-PW91/TZ2P and CCSD(T)/LACV3P++** methods.

atoms used triple-ζ Slater-type orbital (STO) basis sets with two p polarization functions (TZ2P).[94] Relativistic corrections employed the zeroth-order regular approximation (ZORA) method, and the integration level was set to 6.0.

Previously reported M−H bond energies are compared with the new results reported herein.[77] Prior post-Hartree−Fock (CCSD(T))[95] calculations were performed using Gaussian98 and the LACV3P++** relativistic effective core potential and the valence basis set of triple-ζ quality including a set of polarization and diffuse functions. Prior DFT calculations used the Jaguar program and the hybrid density functional B3LYP in association with the built-in LACV3P++** basis set. For consistency with previously reported bond dissociation energies,[77] the reported values are not corrected for zero-point energies or estimated basis set superposition errors.

Geometries of MH_n Complexes. As revealed by the geometric features shown in Table 6, the optimized geometries of MH_n molecules using the SARC all-electron basis sets and DKH or ZORA Hamiltonians conform to those computed previously[89,90] and expected based on a simple hybridization and Lewis-like considerations.[73,74] For example, the structure of WH_6 displays strong deviation from the octahedron predicted by valence shell electron pair repulsion (VSEPR) in favor of C_{3v} point group symmetry with 63° and 117° bond angles as predicted by idealized sd^5 hybridization (Figure 3 and Table 6). All-electron computations with scalar relativistic treatments exhibit M−H bond lengths and charge distributions that are similar to prior computations with relativistic effective core potentials. For example, tetrahedral MH_4 fragments exhibit the following M−H average bond lengths: M = Hf, $R_{Hf-H} = 1.835$ Å and M = Os, $R_{Os-H} = 1.593$ Å for all-electron scalar relativistic treatments compared with values of $R_{Hf-H} = 1.833$ Å and $R_{Os-H} = 1.601$ Å. Similarly, NPA based charges, $Q_{Hf} = +1.77$ and $Q_{Os} = +0.08$, for all-electron computations (Table 7), closely match those, $Q_{Hf} = +1.76$ and $Q_{Os} = +0.12$, determined with effective core potentials. It is interesting to note that different relativistic treatments, DKH and ZORA, have no significant effects on important molecular properties such as molecular geometries, relative energies of different stationary states, charge distributions, and bond dissociation energies. The contraction error of the SARC basis is estimated to be ~0.005 Å for M−H bond distances.

MH_n Bond Dissociation Energies. Simple M−H bond dissociation energies computed exhibit remarkable consistency over the range of computational methods and basis sets reported herein. Within the all-electron calculations using the B3LYP functional, the greatest range of computed bond dissociation energies, 3.05 kcal/mol, occurs for ReH_5. Among seven different calculations of M−H bond dissociation energies for eight metals, the rmsd is 1.81 kcal/mol.

It is interesting to note that relativistic core potential representations and all-electron treatments with scalar relativistic calculations using the B3LYP functional yield similar bond dissociation energies (see Table 8 and Figure 4). This is not surprising in that bond dissociation energies are primarily

Table 9. Equilibrium Geometries (Å), Dissociation Energies (eV), and Spectroscopic Constants (cm^{-1}) of Au Diatomic Molecules[a]

	R_e	D_e	ω_e	$\omega_e x_e$	ref
	AuH				
CCSD(T)/SARC-DKH	1.521	3.31	2307	49.9	
CCSD(T)/SARC-ZORA	1.520	3.33	2312	49.7	
CCSD(T)/AE	1.525	2.92	2288	42	96, 107
CCSD(T)/PP	1.510	3.28	2324		106
DFT-BDF	1.537	3.34	2259		97
DFT-ZORA(MP)	1.537	3.33	2258		97
expt	1.524	3.36	2305		109
	AuF				
CCSD(T)/SARC-DKH	1.932	2.63	551	3.6	
CCSD(T)/SARC-ZORA	1.932	2.63	551	3.6	
CCSD(T)/PP-aVTZ	1.942	2.89	541	2.8	98
CCSD(T)/PP-CBS	1.935	2.97	548	2.8	98
DFT-BDF	1.941	3.48	531		97
DFT-ZORA(MP)	1.948	3.39	526		97
expt	1.918	3.01	564	3.3	99
	AuCl				
CCSD(T)/SARC-DKH	2.226	3.10	371	1.4	
CCSD(T)/SARC-ZORA	2.226	3.08	371	1.4	
CCSD(T)/PP-aVTZ	2.230	2.80	367	1.3	98
CCSD(T)/PP-CBS	2.213	2.96	375	1.3	98
DFT-BDF	2.228	2.96	359		97
DFT-ZORA(MP)	2.247	2.91	352		97
DFT(BP)/PP	2.243	3.00	356		104
expt	2.199	3.13	384	1.5	100
	AuBr				
CCSD(T)/SARC-DKH	2.344	2.75	255	0.7	
CCSD(T)/SARC-ZORA	2.344	2.74	255	0.7	
CCSD(T)/PP-aVTZ	2.346	2.61	256	0.7	98
CCSD(T)/PP-CBS	2.334	2.75	260	0.6	98
DFT-BDF	2.351	2.59	250		97
DFT-ZORA(MP)	2.366	2.70	244		97
expt	2.318	2.96	264	0.7	100
	AuI				
CCSD(T)/SARC-DKH	2.474	3.10	220	0.5	
CCSD(T)/SARC-ZORA	2.474	3.09	220	0.5	
CCSD(T)/PP-aVTZ	2.500	2.48	209	0.5	98
CCSD(T)/PP-CBS	2.487	2.62	211	0.5	98
expt	2.471	2.86	216	0.5	101
	Au_2				
CCSD(T)/SARC-DKH	2.501	2.38	183	0.4	
CCSD(T)/SARC-ZORA	2.500	2.37	183	0.4	
CCSD(T)/PP	2.494	2.18	196		106
cp-CCSD(T)/AE	2.488	2.19	187		108
CCSD(T)/AE-DK3 point-charge	2.484	2.25	192		102
CCSD(T)/AE-DK3 finite-nucleus	2.480	2.31	194		35
DFT(B3LYP)/AE	2.541	2.03	169		104
DFT-BDF	2.513	2.22	183		97
DFT-ZORA(MP)	2.521	2.25	175		97
expt	2.472	2.31	191		109

[a] Spectroscopic constants were obtained in this work by a least-squares fit to a Morse potential.

determined by valence shell interactions. The new contracted basis sets for scalar relativistic calculations retain much of the computational efficiency of the effective core potential calculations but should also prove particularly useful in computing properties that are not accessible with effective potentials, such as hyperfine and quadrupole coupling parameters.

Coupled Cluster Calculations of Au Compounds. In the preceding sections, we established that the SARC basis sets perform excellently in DFT calculations of third-row transition metal species, in terms of both structures and energetics. We now address the question whether the applicability of the SARC basis sets is limited to DFT or whether they can be used in more demanding correlated ab initio approaches. Since coupled-cluster theory at the CCSD(T) level (coupled-cluster with single, double, and perturbative triple excitations) is currently regarded as one of the most reliable and efficient correlated methods in the field of small-molecule applications, we employ it for our study of six diatomic compounds of gold: AuH, AuF, AuCl, AuBr, AuI, and Au_2. CCSD(T) calculations using both DKH2 and ZORA scalar relativistic Hamiltonians are performed on this test set by correlating all valence electrons. Note that since the SARC basis sets were not explicitly designed for correlated calculations, it is advisable to exclude the core and outer-core (4f) electrons from correlation treatments. Otherwise some inaccuracies are introduced that we attribute to the effects of basis set superposition error.

The basis sets used are of TZVPP quality and for Au correspond to the [17s11p8d3f1g] contraction, whereas for the other elements to the appropriate relativistically recontracted Karlsruhe TZVPP basis sets (H (5s2p1d) → [3s2p1d], F (11s6p2d1f) → [6s3p2d1f], Cl (14s9p2d1f) → [8s4p2d1f], Br(17s13p8d1f)→[10s8p4d1f],I(19s15p9d2f)→[12s10p5d2f]). All these molecules have been the subject of numerous experimental and theoretical studies in the past.[35,96–108] The wealth of available data and the volume of existing publications are such that extensive comparisons are prohibitive for our present purposes; thus, we necessarily limit the comparison of the SARC data to only a representative selection of most recent results (Table 9) and direct the reader to the cited literature, especially to the review by Pyykkö,[96] for a comprehensive coverage of the subject.

A striking feature is the remarkable agreement between the DKH and ZORA approaches; this gives us confidence that the SARC basis sets are well-adapted to the individual formalisms and that there are no imbalances in the basis set construction. Looking more closely at the actual data and making comparisons both with previous CCSD(T) results and with experiment, it becomes evident that the present CCSD(T)/SARC results are consistently accurate for all molecules considered. They are clearly superior to the available DFT results, yielding in general bond lengths that are significantly shorter and thus closer to experiment. Crucially, all predicted equilibrium parameters also compare favorably with previous CCSD(T) calculations that employ all-electron basis sets or—more commonly—pseudopotentials, often surpassing them in accuracy. Of special interest for comparison purposes are the gold halides, which have been recently studied by Puzzarini and Peterson using CCSD(T) with systematic sequences of correlation consistent pseudopotential basis sets (the augmented VTZ and projected CBS results are included in Table 9).[98] It is not our intention to establish whether the present CCSD(T)/SARC results are inferior or superior, but from the differences observed between the two approaches, we can safely conclude that the SARC basis

sets perform reliably in the context of scalar relativistic CCSD(T) calculations.

Summary

The contracted basis sets reported herein are constructed for accurate but yet affordable all-electron treatments of third-row transition metal systems in conjunction with scalar relativistic Hamiltonians (DKH or ZORA). In fact, they are sufficiently small to be used in place of effective core potentials (ECPs) for routine studies of molecules. Various metrics, including atomic ionization potentials, molecular geometries, and bond dissociation energies, indicate that the basis sets provide a balanced description of core and valence electron densities. Overall, the level of agreement between ECP based, DKH, and ZORA results for a variety of third-row transition metal species is striking, as is the success of the B3LYP functional upon comparison with either experiment or high level CCSD(T) calculations. Moreover, the excellent results obtained with the SARC basis sets in a series of CCSD(T) calculations of gold compounds confirm that the applicability of the SARC basis sets can be extended to correlated methods as long as a valence-only correlation strategy is followed.

The SARC basis sets are only loosely contracted, and hence, they are computationally more efficient than the generally contracted relativistic basis sets reported by other workers.[33–40] The main field of application for the new basis sets is expected to be calculation of molecular properties for which the core electrons cannot be neglected; for example, in studies of electron paramagnetic resonance, Mössbauer and X-ray absorption spectra. In addition, the SARC basis sets are ideally suited for the derivation of electron densities that will be subsequently subjected to topological analysis: as Frenking has pointed out,[110] total electron densities derived from ECP calculations may lead to artifacts in the topological analysis and therefore scalar relativistic all-electron calculations are to be preferred. It is interesting to note in this context that NBO derived properties appear to be less critical in this respect and showed a remarkable consistency between ECP and scalar relativistic all-electron calculation schemes.

Acknowledgment. D.A.P. and F.N. gratefully acknowledge financial support from the DFG priority program 1137 "Molecular Magnetism".

Supporting Information Available: Full listings of the SARC basis sets. This material is available free of charge via the Internet at http://pubs.acs.org.

References

(1) Kletzin, A.; Adams, M. W. W. *FEMS Microbiol. Rev.* **1996**, *18*, 5.

(2) Hagen, W. R.; Arendsen, A. F. *Struct. Bonding (Berlin)* **1998**, *90*, 161.

(3) Farrell, N. *Uses of Inorganic Chemistry in Medicine*; Royal Society of Chemistry: Cambridge, 1999; p 208.

(4) Koch, W.; Holthausen, M. C. *A Chemist's Guide to Density Functional Theory*, 2nd ed.; Wiley-VCH: Weinheim, 2002; p 528.

(5) Parr, R. G.; Yang, W. *Density-Functional Theory of Atoms and Molecules*; Oxford University Press: Oxford, 1989; p 352.

(6) Pyykkö, P. *Chem. Rev.* **1988**, *88*, 563.

(7) Hay, P. J.; Wadt, W. R. *J. Chem. Phys.* **1985**, *82*, 270.

(8) Hay, P. J.; Wadt, W. R. *J. Chem. Phys.* **1985**, *82*, 299.

(9) Cundari, T. R.; Stevens, W. J. *J. Chem. Phys.* **1993**, *98*, 5555.

(10) Stevens, W. J.; Krauss, M.; Basch, H.; Jasien, P. G. *Can. J. Chem.* **1992**, *70*, 612.

(11) Hurley, M. M.; Pacios, L. F.; Christiansen, P. A.; Ross, R. B.; Ermler, W. C. *J. Chem. Phys.* **1986**, *84*, 6840.

(12) Lajohn, L. A.; Christiansen, P. A.; Ross, R. B.; Atashroo, T.; Ermler, W. C. *J. Chem. Phys.* **1987**, *87*, 2812.

(13) Ross, R. B.; Powers, J. M.; Atashroo, T.; Ermler, W. C.; Lajohn, L. A.; Christiansen, P. A. *J. Chem. Phys.* **1990**, *93*, 6654.

(14) Andrae, D.; Haussermann, U.; Dolg, M.; Stoll, H.; Preuss, H. *Theor. Chim. Acta* **1991**, *78*, 247.

(15) Andrae, D.; Haussermann, U.; Dolg, M.; Stoll, H.; Preuss, H. *Theor. Chim. Acta* **1990**, *77*, 123.

(16) Dolg, M.; Wedig, U.; Stoll, H.; Preuss, H. *J. Chem. Phys.* **1987**, *86*, 866.

(17) Stoll, H.; Metz, B.; Dolg, M. *J. Comput. Chem.* **2002**, *23*, 767.

(18) Dolg, M. Effective core potentials. In *Modern Methods and Algorithms of Quantum Chemistry*, 2 ed.; Grotendorst, J., Ed.; John von Neumann Institute for Computing: Jülich, 2000; Vol. 3, pp 507−540.

(19) Frenking, G.; Antes, I.; Böhme, M.; Dapprich, S.; Ehlers, A. W.; Jonas, V.; Neuhaus, A.; Otto, M.; Stegmann, R.; Veldkamp, A.; Vyboishchikov, S. F. *Rev. Comp. Chem.* **1996**, *8*, 63.

(20) van Lenthe, E.; Snijders, J. G.; Baerends, E. J. *J. Chem. Phys.* **1993**, *99*, 4597.

(21) van Lenthe, E.; Baerends, E. J.; Snijders, J. G. *J. Chem. Phys.* **1994**, *101*, 9783.

(22) van Lenthe, E.; Snijders, J. G.; Baerends, E. J. *J. Chem. Phys.* **1996**, *105*, 6505.

(23) van Wüllen, C. *J. Chem. Phys.* **1998**, *109*, 392.

(24) Dyall, K. G.; van Lenthe, E. *J. Chem. Phys.* **1999**, *111*, 1366.

(25) Douglas, M.; Kroll, N. M. *Ann. Phys.* **1974**, *82*, 89.

(26) Hess, B. A. *Phys. Rev. A* **1985**, *32*, 756.

(27) Hess, B. A. *Phys. Rev. A* **1986**, *33*, 3742.

(28) Jansen, G.; Hess, B. A. *Phys. Rev. A* **1989**, *39*, 6016.

(29) Wolf, A.; Reiher, M.; Hess, B. A. *J. Chem. Phys.* **2002**, *117*, 9215.

(30) Amsterdam Density Functional (ADF); SCM, Theoretical Chemistry, Vrije Universiteit: Amsterdam, The Netherlands. http://www.scm.com (accessed Feb 14, 2008).

(31) te Velde, G.; Bickelhaupt, F. M.; Baerends, E. J.; Guerra, C. F.; Van Gisbergen, S. J. A.; Snijders, J. G.; Ziegler, T. *J. Comput. Chem.* **2001**, *22*, 931.

(32) van Wüllen, C. *J. Comput. Chem.* **1999**, *20*, 51.

(33) Roos, B. O.; Lindh, R.; Malmqvist, P. A.; Veryazov, V.; Widmark, P. O. *J. Phys. Chem. A* **2005**, *109*, 6575.

(34) Balabanov, N. B.; Peterson, K. A. *J. Chem. Phys.* **2005**, *123*, 064107.

(35) Nakajima, T.; Hirao, K. *J. Chem. Phys.* **2002**, *116*, 8270.

(36) Watanabe, Y.; Tatewaki, H.; Koga, T.; Matsuoka, O. *J. Comput. Chem.* **2006**, *27*, 48.

(37) Sekiya, M.; Noro, T.; Miyoshi, E.; Osanai, Y.; Koga, T. *J. Comput. Chem.* **2006**, *27*, 463.

(38) Noro, T.; Sekiya, M.; Osanai, Y.; Koga, T.; Matsuyama, H. *J. Comput. Chem.* **2007**, *28*, 2511.

(39) Faegri, K. *Theor. Chem. Acc.* **2001**, *105*, 252.

(40) Faegri, K. *Chem. Phys.* **2005**, *311*, 25.

(41) Ahlrichs, R.; May, K. *Phys. Chem. Chem. Phys.* **2000**, *2*, 943.

(42) Weigend, F.; Ahlrichs, R. *Phys. Chem. Chem. Phys.* **2005**, *7*, 3297.

(43) Weigend, F.; Furche, F.; Ahlrichs, R. *J. Chem. Phys.* **2003**, *119*, 12753.

(44) Neese, F. *ORCA—an ab initio, Density Functional and Semiempirical Program Package*, 2.6−35; Universität Bonn: Bonn, Germany, 2008.

(45) Strange, P. *Relativistic Quantum Mechanics*; Cambridge University Press: Cambridge, 1998; p 610.

(46) Hess, B. A., Marian, C. M., Jensen, P. , Bunker, P. R. , Eds. Relativistic effects in the calculation of electronic energies. In *Computational Molecular Spectroscopy*; John Wiley & sons: New York, 2000; pp 169−220.

(47) Jensen, H. J. A.; Saue, T.; Visscher, L. Dirac, a relativistic ab initio electronic structure program. http://dirac.chem.sdu.dk (accessed Feb 14, 2008).

(48) Heully, J. L.; Lindgren, I.; Lindroth, E.; Martenssonpendrill, A. M. *Phys. Rev. A* **1986**, *33*, 4426.

(49) Lindroth, E.; Heully, J. L.; Lindgren, I.; Martenssonpendrill, A. M. *J. Phys. B.* **1987**, *20*, 1679.

(50) Filatov, M. *Chem. Phys. Lett.* **2002**, *365*, 222.

(51) Filatov, M.; Cremer, D. *Mol. Phys.* **2003**, *101*, 2295.

(52) Filatov, M.; Cremer, D. *J. Chem. Phys.* **2003**, *118*, 6741.

(53) Filatov, M.; Cremer, D. *Chem. Phys. Lett.* **2003**, *370*, 647.

(54) Filatov, M.; Cremer, D. *J. Chem. Phys.* **2005**, *122*, 044104.

(55) Reiher, M. *Theor. Chem. Acc.* **2006**, *116*, 241.

(56) Wolf, A.; Reiher, M.; Hess, B. A. *J. Chem. Phys.* **2002**, *117*, 9215.

(57) Reiher, M.; Wolf, A. *J. Chem. Phys.* **2004**, *121*, 10945.

(58) Wolf, A.; Reiher, M.; Hess, B. A. *J. Chem. Phys.* **2004**, *120*, 8624.

(59) Neese, F.; Wolf, A.; Fleig, T.; Reiher, M.; Hess, B. A. *J. Chem. Phys.* **2005**, *122*, 204107.

(60) Wolf, A.; Reiher, M. *J. Chem. Phys.* **2006**, *124*, 064103.

(61) Reiher, M.; Wolf, A. *Phys. Lett. A* **2007**, *360*, 603.

(62) Hirata, S.; Yanai, T.; de Jong, W. A.; Nakajima, T.; Hirao, K. *J. Chem. Phys.* **2004**, *120*, 3297.

(63) van Wüllen, C. *Chem. Phys.* **2005**, *311*, 105.

(64) Kutzelnigg, W.; Liu, W. J. *J. Chem. Phys.* **2005**, *123*, 241102.

(65) Kutzelnigg, W.; Liu, W. J. *J. Chem. Phys.* **2006**, *125*, 107102.

(66) Kutzelnigg, W.; Liu, W. J. *Mol. Phys.* **2006**, *104*, 2225.

(67) Reiher, M.; Wolf, A. *J. Chem. Phys.* **2004**, *121*, 2037.

(68) Wolf, A.; Reiher, M. *J. Chem. Phys.* **2006**, *124*, 064102.

(69) Visscher, L.; van Lenthe, E. *Chem. Phys. Lett.* **1999**, *306*, 357.

(70) Huzinaga, S.; Kolbukowski, M. *Chem. Phys. Lett.* **1993**, *212*, 260.

(71) Huzinaga, S.; Miguel, B. *Chem. Phys. Lett.* **1990**, *175*, 289.

(72) Linstrom, P. J.; Mallard, W. G. *NIST Chemistry WebBook, NIST Standard Reference Database Number 69*; National Institute of Standards and Technology: Gaithersburg, MD, 2005.

(73) Weinhold, F.; Landis, C. R. *Valency and Bonding: A Natural Orbital Donor:Acceptor Perspective*; Cambridge University Press: New York, 2005; p 760.

(74) Landis, C. R.; Weinhold, F. *J. Comput. Chem.* **2007**, *28*, 198.

(75) Landis, C. R.; Cleveland, T.; Firman, T. K. *J. Am. Chem. Soc.* **1995**, *117*, 1859.

(76) Landis, C. R.; Firman, T. K.; Root, D. M.; Cleveland, T. *J. Am. Chem. Soc.* **1998**, *120*, 1842.

(77) Uddin, J.; Morales, C. M.; Maynard, J. H.; Landis, C. R. *Organometallics* **2006**, *25*, 5566.

(78) Brunck, T. K.; Weinhold, F. *J. Am. Chem. Soc.* **1979**, *101*, 1700.

(79) Carpenter, J. E.; Weinhold, F. *J. Am. Chem. Soc.* **1988**, *110*, 368.

(80) Foster, J. P.; Weinhold, F. *J. Am. Chem. Soc.* **1980**, *102*, 7211.

(81) Reed, A. E.; Weinstock, R. B.; Weinhold, F. *J. Chem. Phys.* **1985**, *83*, 735.

(82) Reed, A. E.; Weinhold, F. *J. Chem. Phys.* **1985**, *83*, 1736.

(83) Glendening, E. D. ; Badenhoop, J. K.; Reed, A. E.; Carpenter, J. E.; Weinhold, F.; Bohmann, J. A.; Morales, C. M. *NBO 5.0*; Theoretical Chemistry Institute, University of Wisconsin: Madison, WI, 2001; http://www.chem.wisc.edu/∼nbo5 (accessed Feb 14, 2008).

(84) Reed, A. E.; Curtiss, L. A.; Weinhold, F. *Chem. Rev.* **1988**, *88*, 899.

(85) *Amsterdam Density Functional (ADF)*; 2005.01, SCM, Theoretical Chemistry, Vrije Universiteit: Amsterdam, The Netherlands, 2005. http://www.scm.com (accessed Feb 14, 2008).

(86) Baerends, E. J.; Ellis, D. E.; Ros, P. *Chem. Phys.* **1973**, *2*, 41.

(87) te Velde, G.; Baerends, E. J. *J. Comput. Phys.* **1992**, *99*, 84.

(88) Ziegler, T.; Rauk, A.; Baerends, E. J. *Theor. Chim. Acta* **1997**, *43*, 261.

(89) Becke, A. D. *J. Chem. Phys.* **1993**, *98*, 5648.

(90) Lee, C. T.; Yang, W. T.; Parr, R. G. *Phys. Rev. B* **1988**, *37*, 785.

(91) Vosko, S. H.; Wilk, L.; Nusair, M. *Can. J. Phys.* **1980**, *58*, 1200.

(92) Perdew, J. P.; Chevary, J. A.; Vosko, S. H.; Jackson, K. A.; Pederson, M. R.; Singh, D. J.; Fiolhais, C. *Phys. Rev. B* **1992**, *46*, 6671.

(93) Rosen, A.; Lindgren, I. *Phys. Rev.* **1968**, *176*, 114.

(94) Snijders, J. G.; Baerends, E. J.; Vernooijs, P. *Atomic Nucl. Data Tables* **1982**, *26*, 483.

(95) Rittby, M.; Bartlett, R. J. *J. Phys. Chem.* **1988**, *92*, 3033.

(96) Pyykkö, P. *Angew. Chem., Int. Ed.* **2004**, *43*, 4412.

(97) Liu, W.; van Wüllen, C. *J. Chem. Phys.* **1999**, *110*, 3730.

(98) Puzzarini, C.; Peterson, K. A. *Chem. Phys.* **2005**, *311*, 177.

(99) Okabayashi, T.; Nakaoka, Y.; Yamazaki, E.; Tanimoto, M. *Chem. Phys. Lett.* **2002**, *366*, 406.

(100) Evans, C. J.; Gerry, M. C. L. *J. Mol. Spectrosc.* **2000**, *203*, 105.

(101) Reynard, L. M.; Evans, C. J.; Gerry, M. C. L. *J. Mol. Spectrosc.* **2001**, *205*, 344.

(102) Tsuchiya, T.; Abe, M.; Nakajima, T.; Hirao, K. *J. Chem. Phys.* **2001**, *115*, 4463.

(103) O'Brien, L. C.; Elliott, A. L.; Dulick, M. *J. Mol. Spectrosc.* **1999**, *194*, 124.

(104) Han, Y.-K.; Hirao, K. *Chem. Phys. Lett.* **2000**, *324*, 453.

(105) Guichemerre, M.; Chambaud, G.; Stoll, H. *Chem. Phys.* **2002**, *280*, 71.

(106) Lee, H.-S.; Han, Y.-K.; Kim, M. C.; Bae, C.; Lee, Y. S. *Chem. Phys. Lett.* **1998**, *293*, 97.

(107) Kaldor, U.; Hess, B. A. *Chem. Phys. Lett.* **1994**, *230*, 1.

(108) Hess, B. A.; Kaldor, U. *J. Chem. Phys.* **2000**, *112*, 1809.

(109) Huber, H. P.; Herzberg, G. *Constants of diatomic molecules*; Van Nostrand: New York, 1979; p 565

(110) Vyboishchikov, S. F.; Sierraalta, A.; Frenking, G. *J. Comput. Chem.* **1997**, *18*, 416.

CT800047T